Journal of Water Process Engineering 70 (2025) 106968

Contents lists available at ScienceDirect

Journal of Water Process Engineering

journal homepage: www.elsevier.com/locate/jwpe

Acid neutralisation capacity (ANC) of biomass ashes and its potential use for phosphogypsum leachate cleaning

F.J. Soto-Cruz [a,*], S.M. Pérez-Moreno [b], A. Barba-Lobo [b], J.P. Bolívar [b], M. Casas-Ruiz [a], V.M. García [c], M.J. Gázquez [a]

[a] Department of Applied Physics, Marine Research Institute (INMAR), University of Cadiz, Campus de Excelencia Internacional del Mar (CEIMAR), Cádiz, Spain
[b] Research Centre of Natural Resources, Health and the Environment (RENSMA), University of Huelva, Campus de Excelencia Internacional del Mar (CEIMAR), Huelva, Spain
[c] Magnon Green Energy, Huelva, Spain

ARTICLE INFO

Editor: Soroush Abolfathi

Keywords:
Acid neutralisation capacity (ANC)
Biomass ash
Phosphogypsum leachate
Pollutant removal
Alkaline waste valorisation

ABSTRACT

The production of acidic leachates from phosphogypsum (PGL) stacks is a worldwide problem, since high concentrations of pollutants (heavy metals, metalloids, sulphates, and phosphates, among others) can be released to the environment. PGL should therefore be treated before its discharge. The aim of this study was to develop a neutralisation procedure using ashes and slags from a biomass power plant to clean PGL, thus contributing to the circular economy. To assess the acid neutralisation capacity (ANC) of ashes and slags, the neutralisation curves with nitric acid, phosphoric acid, and PGL were performed after adding each waste type. Furthermore, the removal efficiency (RE) of the cleaning treatment for major and trace elements was obtained. The biomass ash demonstrated a greater degree of pollutant removal efficiency (around 100 % for many heavy metals), exhibiting a 20 % improvement over the slags in the neutralisation process. This can be attributed to the higher quartz content and lower specific area observed in the slags, which ultimately resulted in lower ANC. For the PGL neutralisation, the biomass ash had an ANC range between 7.37 mEq/g and 9.79 mEq/g of residue, and the RE for toxic metals was generally >90 %. Finally, when diluting PGL (1/10), the residue could clean all the elemental pollutants considered by the regulations.

1. Introduction

Industrialisation significantly improves people's economy and social level. However, it also produces hazardous waste that can harm the environment and people's health. One of the critical industries for society is food industry, since many raw materials are used as fertilisers and pesticides [1].

Phosphoric acid (PA) is among the main raw materials to manufacture fertilisers, and its production is based on the dissolution of phosphate rock (fluorapatite ($Ca_5(PO_4)_3F$)) by adding diluted sulphuric acid (70 %). This chemical reaction generates both phosphoric acid (aqueous phase) and a white solid waste named phosphogypsum (PG) (Eq. (1)) [2].

$$Ca_5(PO_4)_3F + 5H_2SO_4 + 10H_2O \rightarrow 3H_3PO_4 + 5CaSO_4 2H_2O + HF \quad (1)$$

PG waste has been classified internationally as TENORM (technologically enhanced naturally occurring radioactive material), as its activity concentrations of natural radionuclides are greater than the thresholds set by both the EU Directives [3,4] and the Spanish regulation [5,6]. In addition, it contains several potential contaminants, such as phosphates, fluorides, sulphates, and heavy metals, among others [7–9]. Typically, PG is stacked worldwide in wet stacking [1], generating acid leachates (pH < 2) with potential contaminants that can cause serious environmental pollution and ecological damage if it is not properly handled [10,11]. In fact, PG affects the environment mainly through the leachate path, since, during the long-term accumulation process of PG, the pollutant content in the PGL is much higher than that of PG, and the ecological toxicity of the PGL is much greater than that of PG [12].

In Huelva (in the southwest of Spain), the PA production industry was active from 1965 to 2010, and its five plants were in the vicinity of the estuary formed by the confluence of the Tinto and Odiel rivers. According to previous studies [13,14], approximately 100 Mt. of PG are stored in the piles covering an area of 1000 ha and are very close to the city of Huelva (Fig. S1). The area is divided into 4 zones: Zones 1, 3, and

* Corresponding author.
E-mail address: franciscojavier.soto@uca.es (F.J. Soto-Cruz).

https://doi.org/10.1016/j.jwpe.2025.106968
Received 30 October 2024; Received in revised form 18 December 2024; Accepted 7 January 2025
Available online 13 January 2025

4 have a mean height of 5 m, while Zone 2 has a pyramidal shape with a height of 20 m. Zone 1 was firstly restored and revegetated (between 1990 and 92) by using only a soil layer of 40 cm, while Zone 4 was remediated between 1997 and 2009 by both the government of Huelva and the regional government of Andalusia [13]. Zones 2 and 3 are surrounded by perimeter channels where leachates from PG weathering are collected from the last 10 years, although some outflows are uncontrollably released into the estuarine environment through edge leakages, thus potentially impacting the environment [2,15,16].

Industrial acid effluents are generally cleaned by using alkaline reagents such as limestone ($CaCO_3$), hydrated lime ($Ca(OH)_2$), pebble quicklime or lime (CaO), sodium carbonate (Na_2CO_3), and caustic soda (NaOH), among others [17–19]. Recent studies have assessed the decontamination of phosphogypsum leachates (PGL) by using alkaline reagents such as hydroxides and carbonates of Ba, Ca, Na, and Mg [9,18,20].

However, the constant consumption of the chemical agent and the need to eliminate the leachate may increase operating costs, impairing economic viability. As such, minimising costs for this process entails finding low-cost neutralisation agents with suitable chemical characteristics that are available in significant amounts.

Recent studies have shown the potential of biomass ash as a substitute of traditional reagents [21–25]. Biomass ashes have a high content of alkaline compounds in the form of oxides, hydroxides, and carbonates [26,27]. In addition, biomass ashes could adsorb contaminant elements due to both the high specific surface area and the presence of negatively charged minerals that allow positively charged metallic elements to be adsorbed [26,28].

In addition, the utilisation of biomass ash as a sustainable and renewable resource has the potential to be environmentally benign [29], as it contributes to the circular economy in contrast to commercial reagents.

Compared to traditional reagents, the use of biomass ash has the potential to mitigate the environmental impact and costs of waste disposal by diminishing the volume of waste material directed to landfills. For example, T.Y. Huang et al. concluded that fly ash reused as alkaline reagent (1 t of fly ash replacing 1 t of limestone) in the Waelz process reduced emissions by 30.6 kg eq CO_2/t fly ash [30].

Furthermore, with the recent increase in the cost, acquisition and development of new waste disposal sites, the management of these fly ashes represents a serious problem for the energy generation industry (480 million tons of biomass ash generated worldwide [31]), hence the importance of finding alternative ways of managing fly ash wastes [32].

There are several studies on cleaning acid mine drainage (AMD) by using ashes from thermal processes (biomass or carbon) [22,23,25]. Additionally, with the exception of Millan-Becerro [33], who used column passive methods with six traditional reagents and biomass ash, no study has ever used biomass ash to treat PGL.

Considering the previous facts, and given the limited research on the treatment of PGL [12], the main objective and novelty of this study was to assess the capacity of alkaline ashes from the combustion of biomass for PGL decontamination following an active method.

2. Materials and methods

2.1. Sampling

PGL samples were collected in February 2022 from the perimeter channel of Zone 3 of the Huelva PG stacks. They were filtered using a vacuum system with cellulose nitrate filters of 0.45 μm pore size and 90 mm in diameter. Subsequently, the physicochemical parameters (pH, electrical conductivity (EC), redox potential (ORP), and temperature (T)) were measured using a portable multiparameter (CRISON MM 40+).

The alkaline wastes used in this work (Table S1) were biomass ashes provided by Magnon Green Energy from its operation centre in Huelva. This business group focuses on producing energy from biomass, and its operation centre in Huelva is made up of three plants (HU-50, HU-46, HU-41), with a total capacity of 137 MW and an annual production of over 800 GWh.

The samples were dried at 60 °C until constant weight. Fly ash (FA) samples were sieved in three fractions: fine fraction, "F" (particle size <63 μm); middle fraction, "M" (63 μm < particle size <0.5 mm), and coarse fraction, "C" (particle size >0.5 mm). Bottom ashes were sieved in two fractions using a 4 mm mesh sieve. Only the finest fraction of all residues was used, due to its higher specific area. Likewise, pH, oxidation/reduction potential (Eh), and electrical conductivity were determined at a solid to liquid (S/L) ratio of 1:2.5 (v/v).

2.2. Characterisation techniques

2.2.1. Elemental analysis

The liquid samples were analysed by inductively coupled plasma-mass spectrometry (ICP-MS) (Agilent 7700) and inductively coupled plasma-optical emission spectrometry (ICP-OES) (Jobin Yvon Ultima 2) in the CIDERTA laboratory at the University of Huelva. The solids were digested using four different acids (HF, HCl, HNO_3, and H_2SO_4) and analysed by both ICP-OES (Agilent Axial 730-ES) and ICP-MS (Perkin Elmer Sciex ELAN 9000) in the Activation Laboratories Ltd. (ACTLABS, Ontario, Canada). The presence of anions in the liquid samples was analysed using the ion chromatography 883 Basic IC plus from Metrohm in the CIDERTA laboratory from the University of Huelva. In addition, the major elements were determined by using an X-ray fluorescence (XRF) sequential spectrophotometer PANanalytical (ZETIUM Minerals) in the Central Research Services of the University of Seville, Spain. The criteria employed to calculate the uncertainties can be consulted in [34].

Regarding the quality control of the equipment, a blank reagent, a certified reference material (NIST SRM 1633c (Trace Elements in Coal Fly Ash)), and a triplicate of every tenth sample were introduced, obtaining accuracies of the analytical data ranging from 5 % to 10 %. The criteria used to calculate ion chromatography uncertainties can be found at the CITIUS webpage [35]. Regarding the data processing, the laboratory sent us the data in an Excel sheet, and we organised them to create the figures. Data processing methods were conducted using Excel: all figures and tables were prepared with this software.

2.2.2. Mineralogical analysis

Approximately 2 g of each solid were mixed with 0.24 g (12 % of the total mass) of zincite (ZnO) and ground by using an agate mortar until the mixture was homogeneous. Subsequently, the sample was sieved with a 250 μm sieve. Zincite was added as an internal standard to quantify the amorphous fraction.

Powder samples were mineralogically characterised as performed in the CITIUS using a Bruker X-ray diffractometer (D8 Advance A25). Crystalline mineral phases were identified using the DIFFRAC.EVA software with the PDF4/Mineral database, and phases were quantified according to the Rietveld method [36] using the DIFFRAC.TOPAS software. The calculation of uncertainties of each crystalline phase and amorphous fraction was carried out by using DIFFRAC.TOPAS software.

2.3. Design of experiments

Depending on the PGL used (location, season, etc.) and the different characteristics of the ashes used, both different neutralisation capacities and removal efficiencies could be obtained. Therefore, five neutralisation curves were conducted in order to study the acid neutralisation capacity of the wastes and their removal efficiencies:

- Experiment 1: PGL neutralisation with NaOH
- Experiment 2: 1.5 M Nitric acid neutralisation with biomass ash
- Experiment 3: 0.5 M Phosphoric acid neutralisation with biomass ash
- Experiment 4: PGL neutralisation with biomass ash

- Experiment 5: Diluted PGL (1/10) neutralisation with biomass ash.

Further detailed information regarding the targets for each neutralisation curve is presented in Table S2 of the Supplementary material.

The neutralisation curves were tested as follows: About 150 mL of reference dissolution (1.5 M NaOH, 1.5 M HNO_3, 0.5 M H_3PO_4, PGL and diluted PGL (1/10) with distilled water) were taken, and a constant mass of alkaline material was slowly added in increments of about 0.1 g up to a stable final pH. The solution was continuously stirred, and physicochemical parameters (pH, EC, ORP, and T) were continuously monitored.

The equivalence points were identified by taking the maximum values of the pH derivative, which corresponds to the greatest variation slope, and their midpoints were obtained both by taking the value of half of the equivalence point obtained from the pH derivative curves.

The final solution from PGL neutralisation was filtered with a 0.45 μm pore filter, and the resulting liquid was reserved for the ICP-MS/OES analysis to determine the composition of the final liquid and to calculate the removal efficiency (RE) of each element. Likewise, RE was calculated as the percentage of change in element concentration (Eq. (2)), considering that the volume of PGL was constant during the chemical reactions.

$$RE\ (\%) = \frac{C_i - C_F}{C_i} \times 100 \quad (2)$$

where C_i is the initial concentration of the element in PGL (mg/L), and C_F is the concentration (mg/L) of the element in the liquid phase after the neutralisation curve of PGL with each solid.

In order to carry out the derivate of the pH with respect to the volume of neutraliser/volume of acid, the command gradient of MatLab was employed [37], which allows deriving a set of numerical data with respect to another set of numerical data. Moreover, this command provides more accurate results compared to the command *diff*, since *diff* only carries out the difference between adjacent elements, while *gradient* provides the partial derivative of the dependent variable with respect to each independent variable.

Finally, to test the reproducibility of the experiments, the most complex experiment (FA_F-50 + PGL) was conducted in triplicate. The results showed standard deviations below 2 % for FAF-50/PGL (g/mol), <5 % for pH, and under 20 % for element concentrations. Data support was included in the Supplementary material to show the stability and reliability of the experimental results (see Tables S9 and S10 in Supplementary material). Additionally, a figure was included in the Supplementary material to make the neutralisation reproducibility test more clear (Fig. S6).

3. Results and discussion

3.1. Phosphogypsum leachate characterisation

PGL properties change throughout the year due to the seasonal behaviour of the climate in Huelva, with extreme values between wet and dry seasons [8,38]. This study includes the physicochemical characterisation of PGL from a dry season sample, since it is the most conservative, with the highest concentrations of contaminants.

The pH of PGL (pH < 2) is significantly lower than that of seawater (pH = 7.8–8.0) and the water of the Tinto river estuary (pH = 4.4–6.9), as is shown in Table S3 (see Supplementary material), and falls below the permissible limit for discharges in coastal and transitional waters [39]. The measured EC and Eh values were slightly higher than the background values (30 % and 50 % greater, respectively).

The concentrations of all elements were higher than those in seawater and those allowed for discharge, as can be observed in Table S3 (see Supplementary material). This composition is in agreement with that of previous studies on the PGL of Huelva [2,15,16,40].

3.2. Fly ash (FA) characterisation

3.2.1. Size distribution

After pre-treatment, different size fractions with different proportions were obtained, as indicated in Table 1. In all ashes, a higher proportion (53–74 %) of medium fraction (0.5 mm > F > 63 μm) was obtained. However, a high proportion (46 %) of fly ash from the HU-46 plant (FA-46) was found in the fine fraction (< 63 μm). This could be due to the fact that HU-46 had a boiler and used a biomass that was different from that employed in HU-50 and HU-41. Although the quantity and quality of ashes was strongly influenced by the characteristics of the biomass, this size particle was similar to that of other FA [41].

In regard with the slags, they had a higher proportion (81–92 %) in the fraction lower than 4 mm. However, this fraction was 10 % higher for slag from the HU-46 plant (S-46) compared to the slag from the HU-50 plant (S-50), which could be due to the fact that the boiler in the HU-50 plant had a fluidised bed, whereas combustion took place on a grate in the HU-46 plant. Furthermore, the biomass used in the two plants was different. Both plants were fuelled by agricultural waste, although HU-50 also used forestry waste, and HU-46 was fuelled by olive kernel oil.

3.2.2. Alkalinity

All residues had alkaline properties (pH between 11.6 and 12.7), although slags had lower pH, around one unit of pH (Table 1). Moreover, the physicochemical parameters of the fine and intermediate phases of the ash from the HU-50 plant were measured. The results indicated that the pH level was over 13. Therefore, separating the ash and using the finer part resulted in a higher pH than using the unseparated ash, which is an advantage when used as a neutraliser.

Likewise, pH values were directly related to EC values, i.e. the higher the pH values, the higher the EC values. FA presented higher EC values, thus they constituted solutions with greater dissolved ions. In addition, fly and bottom ashes had positive Eh, resulting in solutions with a reducing character. As a result, FA were more likely to be used as alkali reagents to neutralise acid leachates.

3.2.3. Elemental composition

The main elements of the biomass ashes were Ca (14–25 %), Si (6–22 %), and K (4–11 %) (Fig. S3a). This was consistent with previous studies, where CaO, SiO_2, and K_2O constituted the highest percentage by weight of biomass FA [42,43]. The composition of ash varied depending on both the type of biomass feedstock and the combustion process used [42]. This variability was also in the samples studied, where there were differences in the proportion of the elements: fine FA from HU-50 (FA_F-50) (Ca > Si > K), fine FA from HU-46 (FA_F-46) (Ca > K > Si), fine FA from HU-41 (FA_F-41) (Ca > Si > K), slag from HU-50 (S-50) (Ca > Si > K), and slag from HU-46 (S-46) (Si > Ca > K). The FA from the HU-50 and HU-41 plants (FA-50 and FA-41, respectively) presented a similar composition, since both were fed by forestry and agricultural biomass. However, the FA from the HU-46 plant (FA-46) had a higher potassium content, as olive residue is rich in K [42].

Other elements such as Cl, S, Fe, Al, and Mg were in the ashes in a concentration between 0.75 % and 5 % (Fig. S3a). However, Cl and S contents were negligible in the composition of the slag. The reason was their volatility during the calcination process, which caused that FA collected a greater proportion than the bottom ash.

In the fine fraction (FA_F-50), the major element was calcium (25 %), while the predominant element in the medium fraction (FA_M-50) was silicon (23 %). Girón et al. [44] also found differences in the concentrations of Ca and Si according to the particle size.

The trace elements in the solids were compared with the values of generic reference levels (NGR) in Andalusia defined by Decree 18/2015 (Table S6), which establishes the legal regime applicable to contaminated soils. None of the solids exceeded any level to determine whether an industrial soil was potentially contaminated. A speciation analysis is required to verify whether Cr(IV) exceeds the concentration established

Table 1
Biomass ash characterisation. Size fraction distribution (%) and pH, Elemental composition (% and mg/kg). Major minerals present in the ash (%). N.D. "not detected". N.M. "not measured". Further information is shown in the Supplementary material (Tables S4, S5, S6, S7). Abbreviations are indicated in Table S8 (see Supplementary material).

Biomass ash		FA-50	FA-46	FA-41	S-50	S-46	FA_M-50	FA_F-50	FA_F-46	FA_F-41
Size fraction (F) distribution (%)	F > 0.5 mm	1	1	13	N.M.	N.M.				
	0.5 mm > F > 63 μm	74	53	68	N.M.	N.M.				
	F < 63 μm	25	46	20	N.M.	N.M.				
	F > 4 mm	N.M.	N.M.	N.M.	19	81				
	F < mm	N.M.	N.M.	N.M.	8	92				
pH		12.47	12.73	12.59	12.18	11.65				
Major elements (%)	Ca				21	14	15	25	22	19
	K				4.2	8.3	4.4	5.1	11	5.1
	Si				20	19	23	10	6.1	12
Minor elements (mg/kg)	As				12.0	6.11	40.9	8.20	69.2	14.3
	Cd				0.13	0.06	1.10	N.D.	2.05	0.61
	Cr				407	119	63.0	83.0	126	104
	Cu				233	257	490	182	694	446
	Ni				37.33	49.03	46.0	46.0	50.87	50.47
	Pb				47.1	19.1	109.0	24.0	334	76.5
	Zn				392	71.8	328	110	1670	178
Major minerals	Quartz				43.7 ± 0.7	N.M	56.1 ± 0.5	14.7 ± 0.2	7.41 ± 0.15	19.3 ± 0.2
	Calcite				1.83 ± 0.12	N.M.	1.8 ± 1.8	14.4 ± 0.3	13.8 ± 0.3	16.7 ± 0.3
	Portlandite				N.D.	N.M.	N.D.	7.5 ± 0.3	N.D.	N.D.

by the regulation (Table S6). However, by comparing the trace elements content of the solids with that of the reference soil (Fig. S4), an enrichment of some elements (As, Cd, Cu, Mo, Pb, Zn) was observed in the residues of biomass combustion, being higher in FA than in slag residues. Furthermore, FA-46 presented the highest degree of enrichment, due to the different composition of the biomass used in this plant.

3.2.4. *Mineral composition*

The mineral phases in the solids were identified by XRD, as indicated in Table S7 (see Supplementary material). For the fine fraction of FA, more than half of their composition was amorphous (55 % in FA_F-50, 41 % in FA_M-50, 63 % in FA_F-46, and 57 % in FA_F-41), which is typical in FA [45]. Apart from the amorphous phase, the main constituents of the residues were quartz and calcite. Quartz (SiO_2) was in all waste materials, with a higher proportion in S-50 (~50 %). It was consistent with the Si content of the sample (Table 1). Silica content could come from the sandy bed used in the boiler, but also from minor amounts of soils adhered to the biomass [26]. In FA_F-41, silicon was also in the form of microcline ($K(AlSi_3O_8)$). A high content of calcite ($CaCO_3$) was obtained in the FA (14–23 %), while only 2 % was found in the bottom ash. Previous studies identified this phase in basic ashes [46].

Calcium, as well as other alkaline compounds like potassium, can be found in combustion residues in various chemical forms, such as oxides, hydroxides, and carbonates. However, in biomass ashes from low

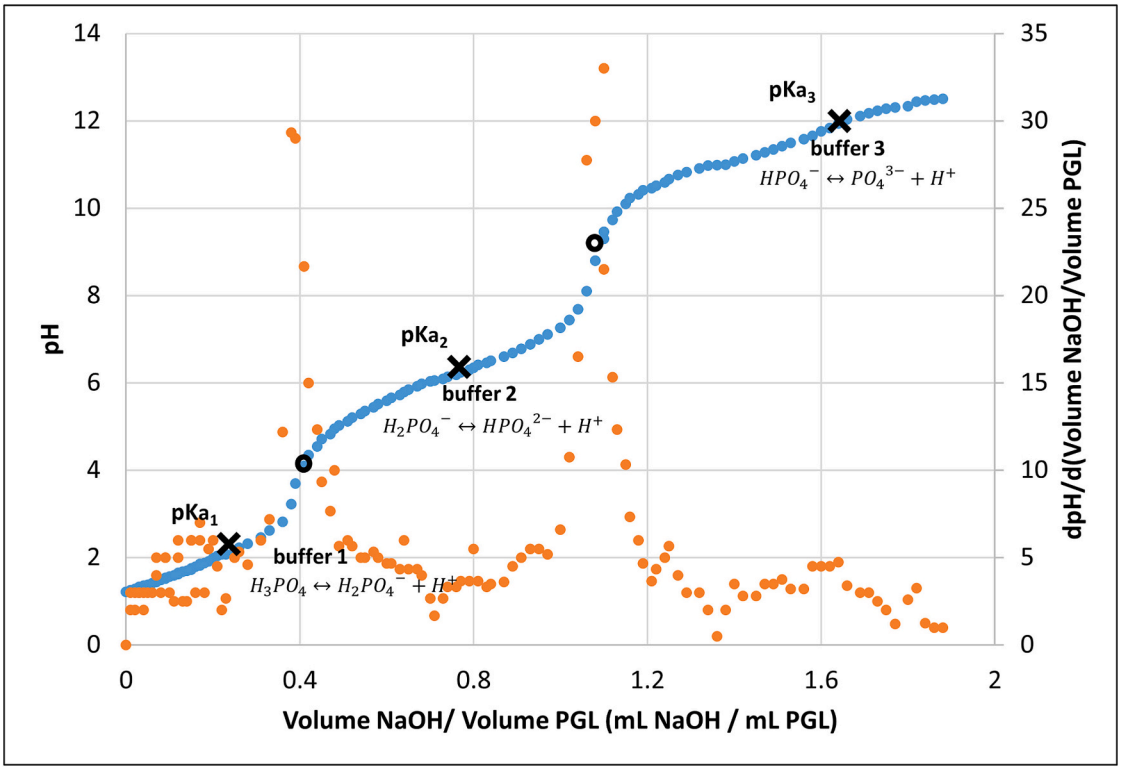

Fig. 1. Titration curve (in blue) of PGL with 1.5 M NaOH and derivative of the titration curve (in orange). Black crosses symbolise midpoints, and black circles symbolise the equivalence points.

temperature combustion (around 500 °C), it tends to be present predominantly in the form of calcium carbonate ($CaCO_3$), while, at high temperatures (around 1000 °C), it is found in the form of oxides. This is due to the temperature at which carbonate decomposition occurs, which starts at around 650 °C for calcium, and 900 °C for potassium [44,47–49]. Carbonate can also be found in biomass residue as a result of the ash weathering in the store process [44]. In addition, calcium could precipitate with other species (e.g. phosphorus) to form phosphate minerals [49], such as ardealite ($HCa_2(PO_4)(SO_4)(H_2O)_4$), which was in FA_F-41 (3 %).

The high potassium content of FA_F-46 was expressed in the mineral phase as syngenite ($K_2Ca(SO_4)_2(H_2O)$) with 10.2 % and as sylvite (KCl) with 5.7 %. The latter mineral was also in FA_F-50 (4.17 %).

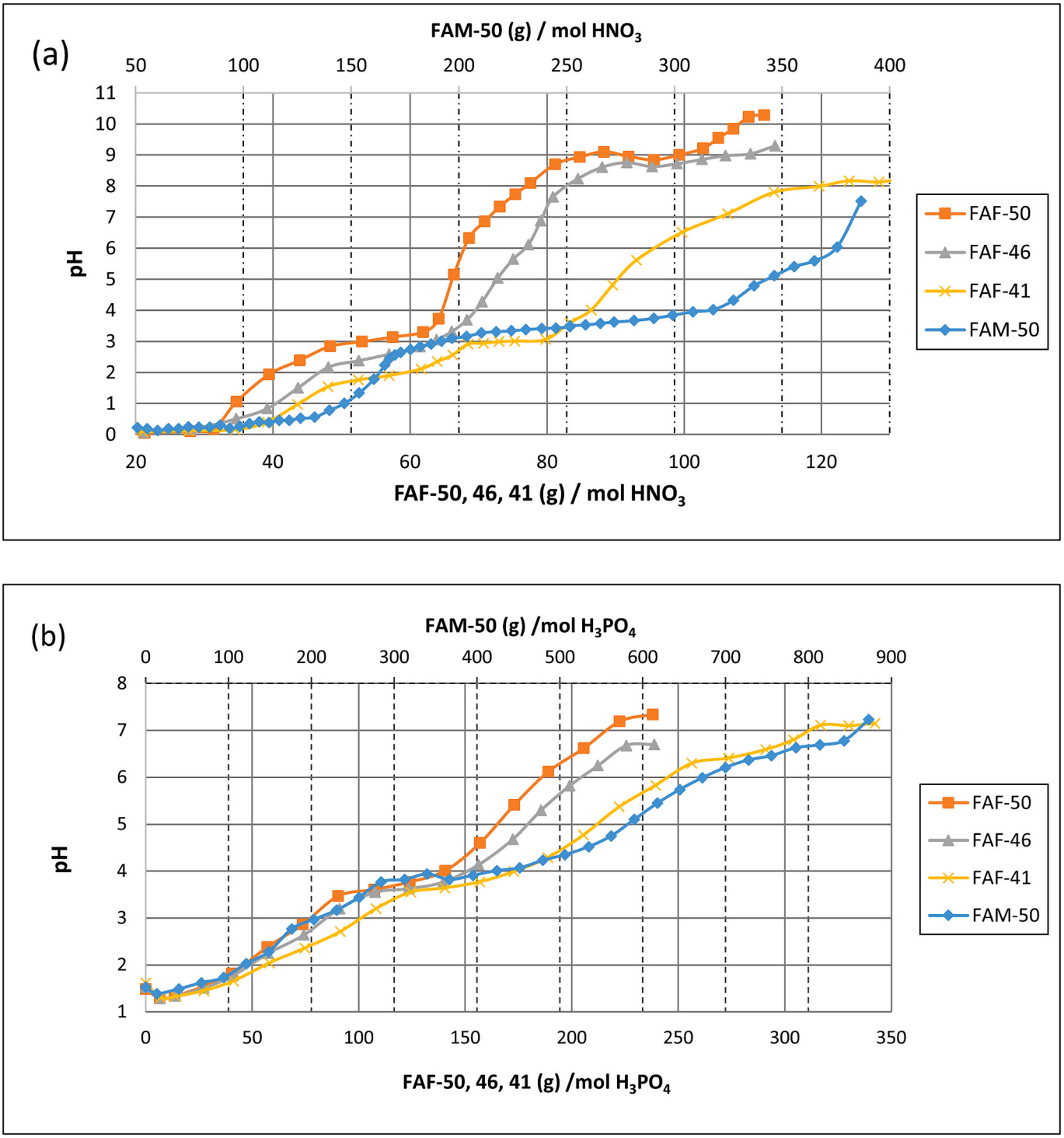

Fig. 2. Neutralisation curves of different acid solutions with biomass fly ashes: (a) nitric acid 1.5 M; (b) phosphoric acid 0.5 M. Abbreviations are indicated in Table S8 (see Supplementary material). Double x-axis represents: at the top, the amount of FA_M-50 per mol of the corresponding acid; at the bottom, the amount of the rest of the FA per mol of the corresponding acid.

3.3. Neutralisation curves

3.3.1. Neutralisation curve of PGL with NaOH

Fig. 1 shows the neutralisation curve of PGL with NaOH. Three buffer zones and two equivalence points were identified in the neutralisation curve. The third equivalence point would be at pH = 14, which corresponds to PO_4^{3-} [50].

Fig. 1 includes the midpoints obtained (taking into account that the third equivalence point would correspond to the PO_4^{3-} from phosphoric acid $pH_{eq} = 14$): $pKa_1 = 2.15$, $pKa_2 = 6.35$, and $pKa_3 = 11.9$. These values were very close to those in pure phosphoric acid ($pKa_1 = 2.2$, $pKa_2 = 7.2$, and $pKa_3 = 12.7$). The dominant acid species in the studied PGL was therefore phosphoric acid (H_3PO_4(aq)), which was expected, since PO_4^{3-} was the anion with the highest concentration (Table S3). This acid was expected to be in PGL, as it was a product formed together with PG in the industrial process of phosphoric acid production (Eq. (1)), thus remnants of it were expected to be present in the PG that was subsequently leached. The concentration of H_3PO_4 was calculated from the equivalence points (pH = 3.7, pH = 9.3). The first equivalence point showed that the H_3PO_4 concentration was 0.83 mol/L, which was very similar to both the P concentration measured by ICP-OES (0.87 mol/L) and the PO_4^- concentration measured by ion chromatography (0.93 mol/L).

Another sub-product from phosphoric acid production expected to be in PGL was hydrofluoric acid (HF (aq)), whose pKa was 3.2, and it was not clearly detected in the neutralisation curve. This was due to the fact that HF was present in lower quantity in the studied sample of PGL than H_3PO_4, where the concentrations of PO_4^- were almost 100 times higher than those of F^-, as indicated in Table S3 (see Supplementary material), which masked the neutralisation of hydrofluoric acid in the neutralisation curve. In contrast, Silvia et al. [20] found HF in the neutralisation curve of PGL from Huelva. This highlights the importance of studying the neutralisation curves for each PGL in each season.

3.3.2. Neutralisation curves of HNO_3 with the biomass ashes

Fig. 2a shows the results of the pH variation of a 1.5 M HNO_3 solution when adding each solid residue. As nitric acid dissociates completely in aqueous solution, its neutralisation curve had no pKa. Instead, the plateaus observed in these curves reflect the ionic species introduced into the solution by the added ashes.

Both fine and intermediate FA showed a plateau at pH = 3, which can be attributed to the dissolution of silicates, as previously reported [51]. Among the ashes, FA_F-50 and FA_F-46 showed a higher ANC than FA_F-41 throughout the curve.

Additionally, the neutralisation curves of FA_F-50 and FA_F-46 were also very similar, with two equivalence points at pH = 2 and two (Fig. S5a–d, see Supplementary material) buffer zones at pH = 3 and 9, possibly due to their shared biomass origin. In contrast, FA_F-41 had a buffer zone at pH = 8. This 8–9 buffer zone may be due to deprotonation (≡Si–OH to ≡Si–O^-) of surface silanol groups present in quartz (SiO_2) [52].

FA_F50 exhibited a higher pH than the other ashes, which may be associated with the portlandite ($Ca(OH)_2$) content, as it is the only ash where this mineral was detected (Table 1). In addition, FA_F-41 showed an extra equivalence point at pH = 3, suggesting the presence of a unique chemical species that was not observed in the other ashes.

The middle fraction of the FA sample (FA_M-50) only showed two equivalence points (Fig. S5a, see Supplementary material) and one pH buffer zone whose midpoints concurred with the fine fraction. However, achieving the same pH values required nearly double the amount of residue. Thus, the most important variable could be the specific surface area (lower in this case), which caused slower reactions. The experiment was stopped at this point by the solution saturation.

3.3.3. Neutralisation curves of H_3PO_4 with residues

Fig. 2b shows the neutralisation curves of a 0.5 M H_3PO_4 solution with each residue. This acid was selected based on the fact that it was expected to be the main acid present in PGL.

In this case, three buffer regions could be deduced from the graphs ($pKa_1 \approx 2$, $pKa_2 \approx 3.6$, and $pKa_3 \approx 7$). These pKa values corresponded to those of phosphoric acid, but they were lower due to the influence of ash.

As can be observed, the amount of mass residue is 3 times greater than that required for the neutralisation with nitric acid, which is logical, since phosphoric acid has $3H^+$.

When the phosphoric acid solution was neutralised, the slopes were smoother than those obtained with nitric acid.

3.3.4. Neutralisation curves of PGL with residues

Neutralisation curves were carried out to determine the necessary amount of alkaline residue to neutralise PGL. Fig. 3a shows the results of the variation of the pH of PGL when adding each solid residue.

As in the previous evaluations, the neutralisation curves of PGL by the fine fraction of FA (FA_F) showed a similar behaviour for all ashes. The FA_F-50 sample was always on top and, therefore, had the highest ANC (Fig. 3a).

At least 3 equivalence points were obtained from the derivative curves in FA (Fig. S5j–l, see Supplementary material). When comparing the medium and fine fraction (FA_M50 and FA_F50) (Fig. S5i–j, see Supplementary material), it can be seen that the third equivalence point (pH = 6) that appears in the fine fraction cannot be observed in the medium fraction, as it does not reach that pH due to the saturation of the solution, although it could also be caused by the fact that there is no detected $Ca(OH)_2$ or CaO in the medium fraction by XRD.

Plateaus around pH = 3.5 and 5.0 were observed for all residues, except for FA_F-41. This might be attributed to the composition, as FA_F-41 was the FA with both the lowest amount of Ca and the highest amount of Si.

For the medium fraction (FA_M-50), the lower curve indicates that a greater amount of residue was required to neutralise the same amount of acid. Additionally, the solution was saturated before reaching the final pH of the fine fractions. As was previously mentioned, this could be due to the lower specific area of the residue.

In the case of the slags, only the neutralisation curves with PGL were carried out. The ANC of these residues was lower than that of FA as it was only possible to reach a pH close to five despite using a large amount of waste, with S-46 being the most effective slag. This could be mainly due to two reasons. Firstly, they had a large proportion of silica, which is an inert material, thus it did not interact with PGL. Secondly, as the particle size is lower, the specific surface area would also be lower, leading to a lower reactivity. In both cases, the plateau at pH = 3.50 was shown again, thus probably it took place by the dissociation of the acid neutralised by the ash that contained species such as $CaCO_3$ (Fig. 3c).

3.3.5. Diluted PGL neutralisation curves with fly ashes

Fig. 3b shows the neutralisation of PGL diluted at 1/10 with FA_F-50 and FA_M-50 compared to the original PGL with FA_F-50 and FA_M-50.

For diluted PGL (1/10), the residues were more effective than for undiluted leachate, as the final pH increased by using both size fractions.

The diluted curve was like the undiluted curve but enlarged. Furthermore, neutralisation with fine fraction required three times less alkaline solid waste per unit of PGL diluted liquid compared to the middle fraction, due to the higher concentration of alkaline species in the fine fraction. Another reason could be that the specific surface area of the fine fraction was greater than that of the middle fraction.

Finally, the diluted PGL reached the same maximum pH (above 8), whereas this was not observed in the concentrated PGL. This difference could be caused by the fact that the alkaline species in the solid were better dissolved, since the solid was not passivated by precipitates that inhibited its action.

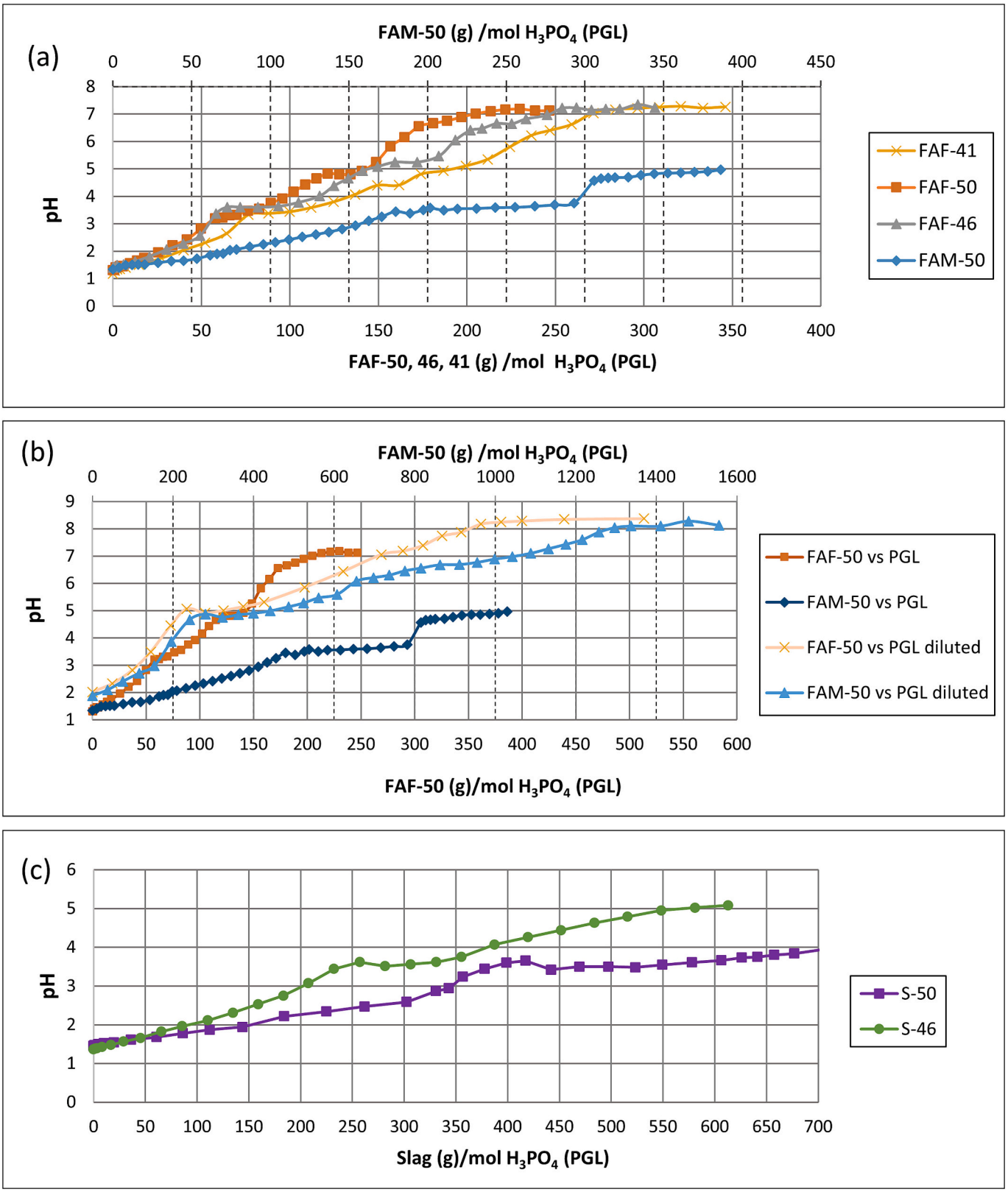

Fig. 3. Neutralisation curves of different acid solutions with biomass fly ashes: (a) H_3PO_4 (PGL); (b) H_3PO_4 (PGL) and diluted H_3PO_4 (PGL) (1/10); (c) H_3PO_4 (PGL). Abbreviations are indicated in Table S8 (see Supplementary material). In (a) and (b), the double x-axis represents: at the top, the amount of FAM-50 per mol of the corresponding acid; at the bottom, the amount of the remaining FA per mol of the corresponding acid.

3.3.6. Acid neutralisation capacity (ANC) of the wastes

ANC was evaluated by considering two cases of final pH, i.e., 5 and 7, as some neutralisations did not reach pH = 7. The obtained ANC for the different experiments is included in Table 2.

The residue with the highest ANC for HNO_3 was FA_F-50 (14.1 mEq/g of residue, at pH = 7), followed by FA_F-46 and FA_F-41, which had an ANC of 12.7 and 10.0 mEq/g at pH = 7, respectively. The FA_M-50 sample showed a significantly lower value (2.58 mEq/g of residue at pH = 7).

The ANC for the neutralisation of H_3PO_4 was lower than that for the neutralisation of HNO_3. The reason could be that phosphoric acid is a weak acid and phosphates precipitate by increasing the pH of the solution. However, the ANC of the residues followed the same behaviour as that shown by nitric acid, with the FA_F-50 sample achieving the highest capacity at pH = 7 (8.99 mEq/g of residue), followed by FA_F-46 (8.38 mEq/g of residue), FA_F-41 (6.31 mEq/g of residue), and FA_M-50 with a lower value (2.29 mEq/g of residue).

For the neutralisation of PGL, the same trend was observed. All FA were effective in achieving a pH around 7, with the FA_F-50 ash being the most effective (ANC = 9.76 mEq/g of residue), followed by FA_F-46 (ANC = 8.15 mEq/g of residue) and FA_F-41 (ANC = 7.37 mEq/g of residue).

Residues neutralised H_3PO_4 better than PGL, mainly due to the difference in their initial concentrations. The H_3PO_4 solution had a concentration of 0.5 M, while PGL had a H_3PO_4 concentration of 0.83 M. Moreover, PGL had other species and ions that precipitated and passivated the solid particles in the residue, making it less soluble and therefore less effective.

Similar results were obtained when diluting the leachate concentration, thus indicating that ANC was not affected by the dilution.

3.4. Removal efficiencies

After completing the neutralisation curves of PGL with the solid residues, the liquids from the neutralisation experiments were analysed by ICP-OES/MS. In this section, the RE of various elements in the liquid phases are shown to analyse the capacity for removing various contaminants from each solid.

3.4.1. Major elements

The major elements with the highest RE for FA neutralisers (FA-50, FA-46, and FA-41) and bottom ashes (S-46 and S-50) were Al, Fe, Ca, and P (RE > 90 %) (Fig. 4a). On the other hand, K and S had higher concentrations in all the liquid phases obtained from the treatments than in the PGL itself, resulting in negative RE values in different ranges (18–240 % for S, and 35–1070 % for K). Many researchers observed that most of the content of K and S in the ash would leach [53,54]. The increase in K and S concentrations in the treated liquid, compared to the initial leachate, can be explained by several chemical interactions and dissolution processes that may occur in systems containing biomass ash and liquids.

As ashes are formed at high temperatures (see Table S1 in the Supplementary material), it is expected that mainly the oxides of the alkaline and alkaline earth elements will be present in proportions that depend on the composition of the biomass. The oxides of the elements can be found in the Supplementary material (see Table S5 in the Supplementary material).

When the ash is mixed with the PGL, the oxides are converted to hydrated oxides (hydroxides), neutralizing the solution and leaving the corresponding alkali metal in solution, unless the solubility product of a salt (e.g., Ca sulphate) is exceeded, in which case the salt of the corresponding element precipitates.

This phenomenon seemed to be the same to explain that the presence of Si was reduced only by FA (within a range of 69–77 %), increasing its concentrations with bottom ashes.

In addition to the aforementioned chemical reactions, other factors may also be involved. One of the possible explanations for this process could be pH-controlled dissolution, although several studies have shown that this effect has no impact on elements such as K or Na [55].

In long-term column leaching tests, initial levels of Na and K in solution are attributed to the dissolution of surface salts, whereas further releases may correspond to the dissolution of the fly ash matrix [54].

In the case of S, due to its dominant surface association in fly ash and the marked solubility of most sulphate-bearing compounds, sulphur is the major soluble element in fly ash, along with Ca [54].

Although not directly addressed in this study, specific experimental conditions (temperature, contact time, liquid-to-solid ratio) also significantly influence dissolution dynamics and chemical reactions. For example, the concentration of K and Na in fly ash leachates has been shown to increase with temperature [56].

The impact of the initial PGL concentration on the RE of the elements was assessed according to grain size by using FA_F-50 and FA_M-50 ashes (Fig. 4b).

Neutralisation of the diluted PGL showed approximately the same RE for Al, Fe, Mg, and P (around 100 %). However, the RE of Ca, Na, K, and S was lower for the fine fraction, thus indicating that these elements dissolved more easily from solid to liquid.

In the case of Ca, it can be seen that there is a negative efficiency in the diluted PGL than in the concentrate, as it is more saturated with Ca sulphate. The Ca in the diluted PGL does not have enough sulphate to reach the solubility product of the $CaSO_4$, and thus remains in solution. This means that the removal efficiency is negative.

The final concentrations with the effluent limits were compared (Table 3), showing that Al and Fe were reduced by both fly and bottom ashes to concentrations suitable for discharge. However, P was only diminished below the limit value by the FA treatment.

For the remaining elements, in the absence of emission limits, seawater values were used as a reference. Concentrations of Ca remained 1 order of magnitude above the reference values for FA, i.e. at the same level as the original leachate. On the contrary, Ca was in the same order of magnitude as seawater for bottom ash and diluted PGL. With regard to K, values increased in 1 or 2 orders of magnitude compared to seawater, but it was in the same order of magnitude when compared to the final leachate of diluted PGL. Likewise, S, Mg, and Na remained in the same order of reference value as initially.

3.4.2. Trace elements

All elements presented a removal >90 % in treatments when using biomass ashes as alkaline reagents, with the exception of As, Cu and Ni

Table 2
ANC of solid wastes for different acid media for two final pH (5 and 7). Not measured: N.M. Abbreviations are indicated in Table S8 (see Supplementary material).

Sample	mEq acid/g solid for pH = 5				mEq acid/g solid for pH = 7			
	HNO_3	H_3PO_4	PGL	Diluted PGL 1/10	HNO_3	H_3PO_4	PGL	Diluted PGL 1/10
FA_F-50	15.1	11.6	14.2	16.4	14.1	8.99	9.76	7.44
FA_M-50	2.89	3.39	5.18	4.53	2.58	2.29	N.M.	1.92
FA_F-46	13.7	10.6	14.2	N.M.	12.7	8.38	8.15	N.M.
FA_F-41	11.2	9	10.7	N.M.	10.0	6.31	7.37	N.M.
S-50	N.M.	N.M.	2.04	N.M.	N.M.	N.M.	N.M.	N.M.
S-46	N.M.	N.M.	3.44	N.M.	N.M.	N.M.	N.M.	N.M.

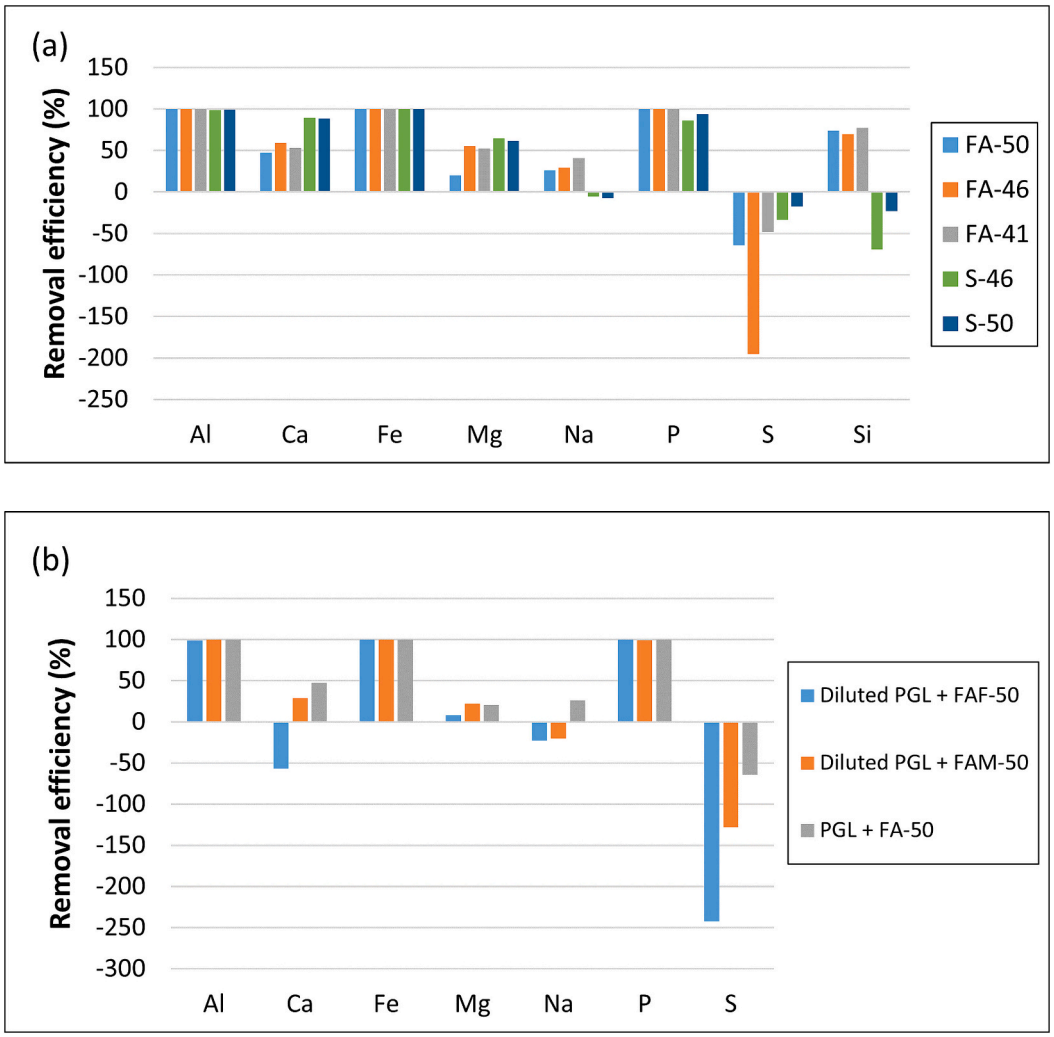

Fig. 4. RE of the major elements (a) in PGL neutralisation with solid wastes, and (b) diluted PGL (1/10) with fine and medium size fraction of FA-50 compared with PGL undiluted with FA-50. Silicon was not measured in either FA_F-50 or FA_M-50 (note: Potassium is not represented due to its high RE values). Abbreviations are indicated in Table S8 (see Supplementary material).

(Fig. 5a).

In the case of As, Pérez-Moreno et al. [20] studied the speciation of this element during alkaline treatment using $Ca(OH)_2$, concluding that, at high alkaline media, there is still a soluble species of As ($CaAsO^-$). This is why, in our previous work, we had to raise the pH up to 12 to obtain a leachate with a concentration of As below the established limit. In addition to the As coming from PGL, the As in solution could come from the ash. Taking into account that the maximum solubility of As is in the pH 7–11 range [54], this element will dissolve into the final solution. In the case of Cu and Ni, they probably come from the PGL itself, since the leachability of these compounds in FA is minimum [54,56].

It is remarkable that, in the case of As, Cd and Ni in the FA, the RE were higher (55 %, 10 % and ~ 20 %, respectively) than in the slags (Table 1), i.e., these elements were not leached and the FA were able to remove a greater proportion of elements than the slags. The opposite occurred in the case of Cu, since, in the slags, Cu was in greater concentrations (Table 1), although they are able to remove more Cu (15 %) from the PLG.

Despite the high RE, when comparing the concentration in the final liquid with the limit values established by Decree 109/2015 (Table 3), it was found that five elements (As, Cd, Cr, Cu and Ni) did not reach suitable concentrations for discharge in coastal waters in the neutralisation with some residues. Excluding As, these elements came from the PGL, as they showed minimum leachability from ash.

Likewise, As and Cd were not suitable under any treatment. In regard with arsenic, neutralisation with FA resulted in concentrations in the same order of magnitude (1.87–2.67 mg/L) as the limit value (1.20 mg/L). The results for bottom ash were 1 order of magnitude greater (61.1–67.7 mg/L). In the case of Cd, the FA achieved a greater removal by exceeding the limit of discharge (0.014 mg/L) with concentrations of the same or 1 higher order of magnitude (0.056–0.225 mg/L), while the concentrations of the slag were 2 orders higher (1.67–1.80 mg/L).

In addition, FA did not achieve optimum values for Cr and Cu. With regard to Cr, differences of about 4 % in RE between ash and slag led to inappropriate values (1.35–2.75 mg/L) greater than those established by the regulation (0.36 mg/L). In relation to Cu, the difference of RE was higher, around 30 %, and the deviation compared to the limit value (0.90 mg/L) was 1 order of magnitude higher (6.18–8.39 mg/L). Furthermore, the slag did not achieve adequate levels of Ni according to regulations (0.72 mg/L), thus achieving a minimum concentration of 2.84 and 5.58 mg/L in the case of PGL + S-46 and PGL + S-50, respectively.

Although some trace elements are pH-dependent, the occurrence in the final solution may be explained by the solubility constant. If there are not enough cations in the solution to achieve the solubility product of the corresponding salt, this potentially toxic anions would still be in solution.

When the neutralisation treatment was carried out with the diluted

Table 3
Major and trace element concentrations (mg/L) in the final leachate obtained during the neutralisation process, and both the Spanish emission limit value in coastal waters (Decree 109/2015) and seawater concentrations. Standard deviation below 20 %. Data rounded to 3 significant figures. Concentrations higher than the emission limit or the seawater value are marked in red. Abbreviations are indicated in Table S8 (see Supplementary material).

	PGL + FA_F-50	PGL + FA_F-46	PGL + FA_F-41	PGL + S-50	PGL + S-46	Diluted PGL + FA_F-50	Diluted PGL + FA_M-50	Point emission limit value	Seawater
Major elements (mg/L)									
Al	<0.04	<0.04	<0.04	2.50	3.40	0.291	<0.04	10.00	
Ca	1130	876	1000	246	222	225	192	Not exist	418
Fe	<0.03	<0.03	<0.03	<0.03	<0.1	<0.1	<0.03	3.6	
K	8700	16,500	5480	1910	5660	916	624	Not exist	445
Mg	2680	1520	1600	1300	1190	805	258	Not exist	1301
Na	10,600	10,100	8510	15,500	15,100	1840	1810	Not exist	10,985
P	11.7	33.7	17.9	1520	3300	11.6	25.3	60	
S	2620	4710	2370	1880	2140	717	477	Not exist	1040
Si	33.9	39.3	29.4	158	217	N.M.	N.M.	Not exist	
Trace elements (mg/L)									
As	1.95	2.67	1.87	61.1	67.7	0.658	1.58	1.20	
Cd	0.225	0.135	0.056	1.67	1.80	<0.001	<0.001	0.014	
Cr	2.75	3.22	1.350	0.212	0.178	0.264	0.080	0.36	
Cu	8.39	7.75	6.18	0.268	0.170	0.0373	0.0220	0.90	
Mn	0.434	0.372	0.375	0.701	0.074	0.027	0.0183	10	
Ni	0.519	0.252	0.287	5.58	2.84	0.0579	0.0440	0.72	
Pb	$2.66{\cdot}10^{-3}$	$5.84{\cdot}10^{-3}$	<0.001	<0.001	<0.001	<0.001	<0.001	0.26	
Se	N.M.	N.M.	N.M.	0.189	0.17	0.033	0.020	0.20	
Th	$2{\cdot}10^{-6}$	$1.59{\cdot}10^{-4}$	<0.0025	<0.0025	<0.0025	<0.0025	<0.0025	Not exist	$3.4{\cdot}10^{-4}$
Ti	0.310	0.50	<0.005	0.066	0.08	<0.005	<0.005	5.0	
U	$1.15{\cdot}10^{-3}$	$5.1{\cdot}10^{-3}$	$1.19{\cdot}10^{-3}$	<0.005	0.008	0.0114	<0.005	Not exist	$2.21{\cdot}10^{-3}$
Zn	0.015	0.189	0.143	0.057	0.0224	0.0604	0.0080	1.80	

PGL (1/10), all the final concentrations were within the limits of the point discharge emissions for FA_F-50 (Table 3). This may not only be explained by the dilution, but also by the fact that now there are less anions to react with the same cations present in the ash. It is worth noting that the RE of As and Th decreased from 98 to 91 % and from 99 to 30 %, respectively, with the diluted leachate and the FA_F-50 ash. On the other hand, the RE of Cu increased from 68 to 99 % with the diluted leachate (Fig. 5b). Similar results were obtained when using the middle fraction.

As was previously mentioned for the major elements, other factors not contemplated in this study such as temperature, L/S ratio and contact time may also be involved.

Traditional methods ($Ca(OH)_2$ and $CaCO_3$) achieve high pH values (pH = 12–13), resulting in removal efficiencies close to 100 % for most toxic elements. In this case, an additional step is currently being introduced for each type of biomass ash to achieve a higher pH by using $Ca(OH)_2$ following the methodology of our previous study [34]. This adjustment enhances the removal of elements that precipitate at higher pH levels, such as arsenic. As a result, potentially harmful elements are transferred into the solid phase.

The management of the solid fraction has two options: landfill disposal or valorisation. Accurate characterisation and leaching tests are essential to evaluate the possibility of recycling the solids [34]. If recycling is not viable (due to environmental, technical or economic factors), it is crucial to determine whether they meet the criteria for safe disposal in landfills.

4. Conclusions

The results of this study provide significant insights into the potential of biomass ashes as an effective neutralizing agent for treating phosphogypsum leachate (PGL). The main findings are as follows:

1. Three FA and two slags from a biomass energy production plant were characterised. Crystalline phases included quartz (7.4–56.1 %) and calcite (1.8–16.7 %) with over 50 % amorphous material in all samples. The major elements were Ca, K, and Si (4.4–23 %), trace elements included Cu (180–490 mg/kg) and Zn (72–1670 mg/kg).
2. The neutralisation curve with NaOH confirmed that phosphoric acid is the dominant acid in the PGL.
3. The neutralisation curves of nitric acid, phosphoric acid, and PGL revealed that fly ashes outperformed slags, with slags showing 20 % lower acid neutralisation capacity (ANC) due to their lower grain specific surface and higher quartz content.
4. The fine fraction (< 63 um) from the HU-50 plant exhibited the highest ANC, making it the most efficient for neutralisation and pollutant removal.
5. Treating PGL with biomass ash led to high removal efficiencies in most elements (> 90 %), except Ca, K, Mg, Na, S, Si, and Cu. Although the removal efficiencies were high, As, Cd, Cr, Cu, Ni and P exceeded the discharge limits set by the regulations.
6. Diluting PGL (1/10) did not affect ANC (± 15 %). However, the liquid resulting from the treatment with FA_F-50 met all discharge requirements according to current regulations.
7. Future research should focus on reaching a greater pH to obtain pollutant removal close to 100 %, ensuring all pollutants are within discharge limits, while addressing the environmental risks associated with transferring harmful elements to the solid phase. Key variables such as temperature, kinetics, stoichiometry and PGL and ash composition should be studied. Advanced characterisation and leaching tests will be critical in evaluating the potential for recycling or safe disposal, paving the way for more sustainable waste management solutions.

CRediT authorship contribution statement

F.J. Soto-Cruz: Writing – review & editing, Writing – original draft, Validation, Software, Methodology, Investigation, Formal analysis, Data curation. **S.M. Pérez-Moreno:** Writing – review & editing, Supervision, Methodology, Investigation, Conceptualization. **A. Barba-Lobo:** Writing – review & editing, Supervision, Methodology, Investigation, Conceptualization. **J.P. Bolívar:** Writing – review & editing, Supervision, Resources, Project administration, Funding acquisition, Conceptualization. **M. Casas-Ruiz:** Supervision, Resources, Project administration, Funding acquisition, Conceptualization. **V.M. García:** Visualization, Supervision, Resources. **M.J. Gázquez:** Writing – review

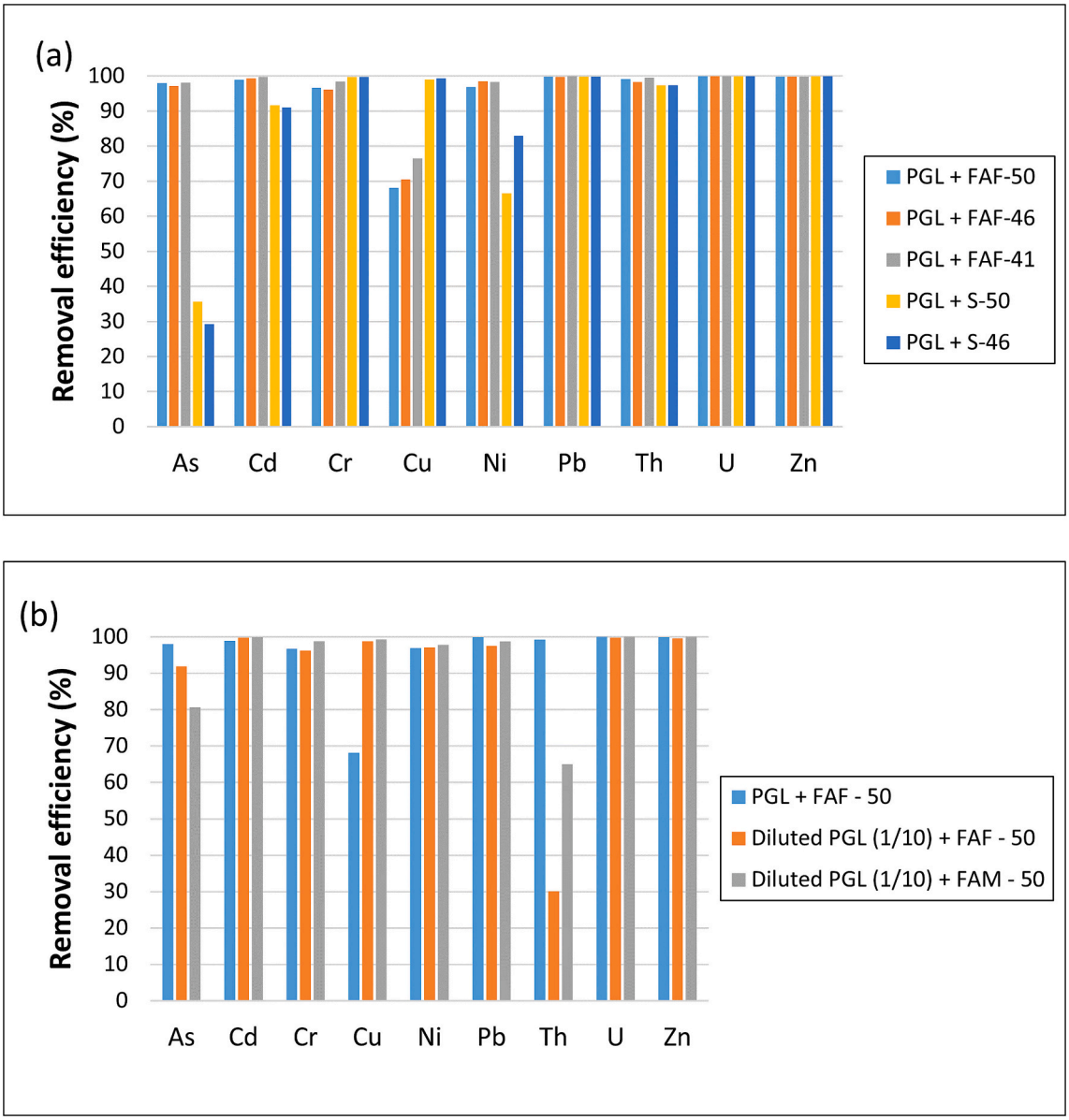

Fig. 5. RE (%) of the trace elements in PGL neutralisation with different biomass wastes (a). RE (%) of minor elements in PGL and diluted PGL (1/10) neutralisation with fine and middle fraction FA-50 (b).

& editing, Supervision, Resources, Project administration, Funding acquisition, Conceptualization.

Declaration of competing interest

The authors declare that they have no known competing financial interests or personal relationships that could have appeared to influence the work reported in this paper.

Acknowledgements

This research was funded by the following projects: Operative FEDER Program-Andalucía 2014-2020 (UHU-1255876, UHU-202020); Grants PID2020-116461RB-C21 and 116461RA-C22 funded by MICIU/AEI/10.13039/501100011033; Research grant UCA/REC44VPCT/2021, by the Universidad de Cádiz; Andalusian government (I+D+i-JAPAIDI-Retos project PY20_00096); Grant TED2021-130361B-I00 funded by MICIU/AEI/10.13039/501100011033 and, by "European Union Next-GenerationEU/PRTR", and Campus de Excelencia Internacional del Mar (CEIMAR) (research project CEIJ-C07.2). The open access fee was co-funded by the QUALIFICA Project (QUAL21-0019, Junta de Andalucía). The authors thank Fertiberia S.A. for their support in obtaining the water samples used in this study. The authors also thank Magnon Green Energy for their support obtaining the ash samples used in this study.

Appendix A. Supplementary data

Supplementary data to this article can be found online at https://doi.org/10.1016/j.jwpe.2025.106968.

Data availability

Data will be made available on request.

References

[1] F. Akfas, A. Elghali, A. Aboulaich, M. Munoz, M. Benzaazoua, J.L. Bodinier, Exploring the potential reuse of phosphogypsum: a waste or a resource? Sci. Total

Environ. 908 (2024) 168196 https://doi.org/10.1016/J.SCITOTENV.2023.168196.
[2] S.M. Pérez-Moreno, M.J. Gázquez, R. Pérez-López, I. Vioque, J.P. Bolívar, Assessment of natural radionuclides mobility in a phosphogypsum disposal area, Chemosphere 211 (2018) 775–783, https://doi.org/10.1016/J.CHEMOSPHERE.2018.07.193.
[3] Council of the European Union, Council Directive 2013/59/Euratom of 5 December 2013 Laying Down Basic Safety Standards for Protection Against the Dangers Arising From Exposure to Ionising Radiation, and Repealing Directives 89/618/Euratom, 90/641/Euratom, 96/29/Euratom, 97/43/Euratom a, 2013.
[4] B. Bouargane, S.M. Pérez-Moreno, A. Barba-Lobo, B. Bakiz, A. Atbir, J. Pedro Bolívar, Behavior of heavy metals and natural radionuclides along the Moroccan phosphogypsum carbonation process with several alkaline reagents, Chem. Eng. Sci. 280 (2023) 119013, https://doi.org/10.1016/J.CES.2023.119013.
[5] Royal Decree 1029/2022, Regulation on health protection against risks derived from exposure to ionizing radiation (in Spanish), Spain, 2022. https://www.boe.es/eli/es/rd/2022/12/20/1029.
[6] Instruction IS-33, From the Nuclear Safety Council on Radiological Criteria for Protection Against the Natural Radiation, 2011 (in Spanish, Spain).
[7] J.M. Abril, R. García-Tenorio, G. Manjón, Extensive radioactive characterization of a phosphogypsum stack in SW Spain: 226Ra, 238U, 210Po concentrations and 222Rn exhalation rate, J. Hazard. Mater. 164 (2009) 790–797, https://doi.org/10.1016/J.JHAZMAT.2008.08.078.
[8] R. Millán-Becerro, R. Pérez-López, C.R. Cánovas, F. Macías, R. León, Phosphogypsum weathering and implications for pollutant discharge into an estuary, J. Hydrol. 617 (2023) 128943, https://doi.org/10.1016/J.JHYDROL.2022.128943.
[9] S.M. Pérez Moreno, C. Romero, J.L. Guerrero, A. Barba-Lobo, M. Gázquez, J.P. Bolívar, Evolution of the waste generated along the cleaning process of phosphogypsum leachates, J. Environ. Chem. Eng. 11 (2023) 111485. doi:https://doi.org/10.1016/J.JECE.2023.111485.
[10] M. Meng, W. Luo, S. Wang, G. Zeng, Predicting the leachate generation from wet phosphogypsum stack using a water-balance-analysis based model, Environ. Res. 212 (2022) 113338, https://doi.org/10.1016/j.envres.2022.113338.
[11] J.L. Guerrero, I. Gutiérrez-Álvarez, F. Mosqueda, M.J. Gázquez, R. García-Tenorio, M. Olías, J.P. Bolívar, Evaluation of the radioactive pollution in the salt-marshes under a phosphogypsum stack system, Environ. Pollut. 258 (2020) 113729, https://doi.org/10.1016/J.ENVPOL.2019.113729.
[12] F. Wu, The treatment of phosphogypsum leachate is more urgent than phosphogypsum, Environ. Res. 262 (2024) 119849, https://doi.org/10.1016/J.ENVRES.2024.119849.
[13] J.L. Mas, E.G. San Miguel, J.P. Bolívar, F. Vaca, J.P. Pérez-Moreno, An assay on the effect of preliminary restoration tasks applied to a large TENORM wastes disposal in the south-west of Spain, Sci. Total Environ. 364 (2006) 55–66, https://doi.org/10.1016/J.SCITOTENV.2005.11.006.
[14] J.L. Guerrero, S.M. Pérez-Moreno, I. Gutiérrez-Álvarez, M.J. Gázquez, J.P. Bolívar, Behaviour of heavy metals and natural radionuclides in the mixing of phosphogypsum leachates with seawater, Environ. Pollut. 268 (2021), https://doi.org/10.1016/J.ENVPOL.2020.115843.
[15] E.M. Papaslioti, R. Pérez-López, A. Parviainen, F. Macías, A. Delgado-Huertas, C. J. Garrido, C. Marchesi, J.M. Nieto, Stable isotope insights into the weathering processes of a phosphogypsum disposal area, Water Res. 140 (2018) 344–353, https://doi.org/10.1016/J.WATRES.2018.04.060.
[16] R. Pérez-López, F. Macías, C.R. Cánovas, A.M. Sarmiento, S.M. Pérez-Moreno, Pollutant flows from a phosphogypsum disposal area to an estuarine environment: an insight from geochemical signatures, Sci. Total Environ. 553 (2016) 42–51, https://doi.org/10.1016/J.SCITOTENV.2016.02.070.
[17] Z. Zhou, Y. Lu, W. Zhan, L. Guo, Y. Du, T.C. Zhang, D. Du, Four stage precipitation for efficient recovery of N, P, and F elements from leachate of waste phosphogypsum, Miner. Eng. 178 (2022) 107420, https://doi.org/10.1016/J.MINENG.2022.107420.
[18] Y. Zhou, G. Zheng, Z. Liu, R. Liu, C. Tao, Multi-stage precipitation for the eco-friendly treatment of phosphogypsum leachates using hybrid alkaline reagents, J. Water Process Eng. 53 (2023) 103626, https://doi.org/10.1016/J.JWPE.2023.103626.
[19] G. Kaur, S.J. Couperthwaite, B.W. Hatton-Jones, G.J. Millar, Alternative neutralisation materials for acid mine drainage treatment, J. Water Process Eng. 22 (2018) 46–58, https://doi.org/10.1016/J.JWPE.2018.01.004.
[20] S.M. Pérez-Moreno, C. Romero, J.L. Guerrero, M.J. Gázquez, J.P. Bolívar, Development of a process for the removal of natural radionuclides and other stable pollutants from acid phosphogypsum stacks leachates, J. Environ. Chem. Eng. 11 (2023) 109032, https://doi.org/10.1016/J.JECE.2022.109032.
[21] B. Prasad, H. Kumar, Treatment of acid mine drainage using a fly ash zeolite column, Mine Water Environ. 35 (2016) 553–557, https://doi.org/10.1007/s10230-015-0373-1.
[22] A. Qureshi, Y. Jia, C. Maurice, B. Öhlander, Potential of fly ash for neutralisation of acid mine drainage, Environ. Sci. Pollut. Res. 23 (2016) 17083–17094, https://doi.org/10.1007/S11356-016-6862-3/FIGURES/4.
[23] M. Roulia, D. Alexopoulos, G. Itskos, C. Vasilatos, Lignite fly ash utilization for acid mine drainage neutralization and clean-up, Clean. Mater. 6 (2022) 100142, https://doi.org/10.1016/J.CLEMA.2022.100142.
[24] Y. Yan, Q. Li, J. Yang, S. Zhou, L. Wang, N. Bolan, Evaluation of hydroxyapatite derived from flue gas desulphurization gypsum on simultaneous immobilization of lead and cadmium in contaminated soil, J. Hazard. Mater. 400 (2020) 123038, https://doi.org/10.1016/J.JHAZMAT.2020.123038.
[25] B.J. Priatmadi, M. Septiana, R. Mulyawan, A.R. Saidy, Increases in pH of acid mine drainage with coal fly-ash application, in: IOP Conference Series: Earth and Environmental Science, 2022: p. 012020. doi:https://doi.org/10.1088/1755-1315/976/1/012020.
[26] S.V. Vassilev, D. Baxter, L.K. Andersen, C.G. Vassileva, An overview of the composition and application of biomass ash. Part 1. Phase–mineral and chemical composition and classification, Fuel 105 (2013) 40–76, https://doi.org/10.1016/J.FUEL.2012.09.041.
[27] R.M. Novais, M.P. Seabra, J.A. Labrincha, Porous geopolymer spheres as novel pH buffering materials, J. Clean. Prod. 143 (2017) 1114–1122, https://doi.org/10.1016/J.JCLEPRO.2016.12.008.
[28] A. Agarwal, U. Upadhyay, I. Sreedhar, S.A. Singh, C.M. Patel, A review on valorization of biomass in heavy metal removal from wastewater, J. Water Process Eng. 38 (2020) 101602, https://doi.org/10.1016/J.JWPE.2020.101602.
[29] O.J. Olatoyan, M.A. Kareem, A.U. Adebanjo, S.O.A. Olawale, K.T. Alao, Potential use of biomass ash as a sustainable alternative for fly ash in concrete production: a review, Hybrid Adv. 4 (2023) 100076, https://doi.org/10.1016/J.HYBADV.2023.100076.
[30] T.Y. Huang, P.T. Chiueh, S.L. Lo, Life-cycle environmental and cost impacts of reusing fly ash, Resour. Conserv. Recycl. 123 (2017) 255–260, https://doi.org/10.1016/J.RESCONREC.2016.07.001.
[31] C. Viegas, C. Nobre, A. Mota, C. Vilarinho, L. Gouveia, M. Gonçalves, A circular approach for landfill leachate treatment: chemical precipitation with biomass ash followed by bioremediation through microalgae, J. Environ. Chem. Eng. 9 (2021) 105187, https://doi.org/10.1016/J.JECE.2021.105187.
[32] R.P. Girón, B. Ruiz, E. Fuente, R.R. Gil, I. Suárez-Ruiz, Properties of fly ash from forest biomass combustion, Fuel 114 (2013) 71–77, https://doi.org/10.1016/J.FUEL.2012.04.042.
[33] R. Millán-Becerro, R. Pérez-López, F. Macías, C.R. Cánovas, Design and optimization of sustainable passive treatment systems for phosphogypsum leachates in an orphan disposal site, J. Environ. Manag. 275 (2020) 111251, https://doi.org/10.1016/J.JENVMAN.2020.111251.
[34] F.J. Soto-Cruz, S.M. Pérez-Moreno, E. Ceccotti, A. Barba-Lobo, J.P. Bolívar, M. Casas-Ruiz, M.J. Gázquez, Valorisation diagnosis of waste from the decontamination of phosphogypsum leachates through a combined calcium carbonate/hydroxide process, Heliyon 10 (2024) e30610, https://doi.org/10.1016/J.HELIYON.2024.E30610.
[35] CITIUS, X-ray laboratory webpage. https://citius.us.es/web/servicio.php?s=lrx#equipo, 2023.
[36] H.M. Rietveld, A profile refinement method for nuclear and magnetic structures, J. Appl. Crystallogr. 2 (1969) 65–71, https://doi.org/10.1107/s0021889869006558.
[37] MatLab, Gradient. https://es.mathworks.com/help/matlab/ref/gradient.html, 2024.
[38] J.L. Guerrero, I. Gutiérrez-Álvarez, A. Hierro, S.M. Pérez-Moreno, M. Olías, J. P. Bolívar, Seasonal evolution of natural radionuclides in two rivers affected by acid mine drainage and phosphogypsum pollution, Catena 197 (2021) 104978, https://doi.org/10.1016/J.CATENA.2020.104978.
[39] Decree 109/2015, Regulations for Discharges into the Hydraulic Public Domain and the Maritime-Terrestrial Public Domain of Andalusia (in Spanish), 2015.
[40] J.P. Bolívar, J.E. Martín, R. García-Tenorio, J.P. Pérez-Moreno, J.L. Mas, Behaviour and fluxes of natural radionuclides in the production process of a phosphoric acid plant, Appl. Radiat. Isot. 67 (2009) 345–356, https://doi.org/10.1016/J.APRADISO.2008.10.012.
[41] R. Rajamma, R.J. Ball, L.A.C. Tarelho, G.C. Allen, J.A. Labrincha, V.M. Ferreira, Characterisation and use of biomass fly ash in cement-based materials, J. Hazard. Mater. 172 (2009) 1049–1060, https://doi.org/10.1016/J.JHAZMAT.2009.07.109.
[42] S.V. Vassilev, D. Baxter, L.K. Andersen, C.G. Vassileva, An overview of the chemical composition of biomass, Fuel 89 (2010) 913–933, https://doi.org/10.1016/J.FUEL.2009.10.022.
[43] G. Zając, J. Szyszlak-Bargłowicz, W. Gołębiowski, M. Szczepanik, Chemical characteristics of biomass ashes, Energies 11 (2018) 2885, https://doi.org/10.3390/en11112885.
[44] R.P. Girón, I. Suárez-Ruiz, B. Ruiz, E. Fuente, R.R. Gil, Fly ash from the combustion of forest biomass (Eucalyptus globulus bark): composition and physicochemical properties, Energy Fuel 26 (2012) 1540–1556, https://doi.org/10.1021/ef201503u.
[45] S.S. Alterary, N.H. Marei, Fly ash properties, characterization, and applications: a review, J. King Saud Univ. - Sci. 33 (2021) 101536, https://doi.org/10.1016/J.JKSUS.2021.101536.
[46] D. Boström, N. Skoglund, A. Grimm, C. Boman, M. Öhman, M. Broström, R. Backman, Ash transformation chemistry during combustion of biomass, in: Energy and Fuels, American Chemical Society, 2012, pp. 85–93, https://doi.org/10.1021/ef201205b.
[47] A. Demeyer, J.C. Voundi Nkana, M.G. Verloo, Characteristics of wood ash and influence on soil properties and nutrient uptake: an overview, Bioresour. Technol. 77 (2001) 287–295, https://doi.org/10.1016/S0960-8524(00)00043-2.
[48] M.K. Misra, K.W. Ragland, A.J. Baker, Wood ash composition as a function of furnace temperature, Biomass Bioenergy 4 (1993) 103–116, https://doi.org/10.1016/0961-9534(93)90032-Y.
[49] T. Sano, S. Miura, H. Furusawa, S. Kaneko, T. Yoshida, T. Nomura, S. Ohara, Composition of inorganic elements and the leaching behavior of biomass combustion ashes discharged from wood pellet boilers in Japan, J. Wood Sci. 59 (2013) 307–320, https://doi.org/10.1007/S10086-013-1337-3/FIGURES/3.

[50] Alexander V. Panov, Practical mitochondriology pitfalls and problems in studies of mitochondria with a description of mitochondrial functions. https://www.researchgate.net/publication/269763545_PRACTICAL_MITOCHONDRIOLOGY_Pitfalls_and_Problems_in_Studies_of_mitochondria_with_a_Description_of_Mitochondrial_Functions, 2014.
[51] N. Petronijević, D. Radovanović, M. Štulović, M. Sokić, G. Jovanović, Ž. Kamberović, S. Stanković, S. Stopic, A. Onjia, Analysis of the mechanism of acid mine drainage neutralization using fly ash as an alternative material: a case study of the extremely acidic Lake Robule in eastern Serbia, Water (Switzerland). 14 (2022) 3244, https://doi.org/10.3390/W14203244/S1.
[52] K. Yuan, N. Rampal, S. Irle, L.J. Criscenti, S.S. Lee, S. Adapa, A.G. Stack, Variations in proton transfer pathways and energetics on pristine and defect-rich quartz surfaces in water: insights into the bimodal acidities of quartz, J. Colloid Interface Sci. 666 (2024) 232–243, https://doi.org/10.1016/J.JCIS.2024.03.144.
[53] L. Tosti, A. van Zomeren, J.R. Pels, J.J. Dijkstra, R.N.J. Comans, Assessment of biomass ash applications in soil and cement mortars, Chemosphere 223 (2019) 425–437, https://doi.org/10.1016/J.CHEMOSPHERE.2019.02.045.
[54] M. Izquierdo, X. Querol, Leaching behaviour of elements from coal combustion fly ash: an overview, Int. J. Coal Geol. 94 (2012) 54–66, https://doi.org/10.1016/J.COAL.2011.10.006.
[55] Y. Zhang, B. Cetin, W.J. Likos, T.B. Edil, Impacts of pH on leaching potential of elements from MSW incineration fly ash, Fuel 184 (2016) 815–825, https://doi.org/10.1016/J.FUEL.2016.07.089.
[56] A. Ugurlu, Leaching characteristics of fly ash, Environ. Geol. 46 (2004) 890–895, https://doi.org/10.1007/S00254-004-1100-6/TABLES/5.